Fast Amplification and Spectral-coded Tags for Strip-based Target Readout with Intelligent Processing (FAST-STRIP)

Introduction

The recent COVID-19 pandemic unequivocally underscored the indispensable role of real-time Polymerase Chain Reaction (PCR) as the gold standard for reliable pathogen diagnosis. However, it also painfully exposed the inherent limitations of centralized PCR testing under conditions of extreme healthcare system stress, leading to substantial delays in booking tests and obtaining critical results. This global health crisis, therefore, spurred significant innovation within the diagnostics industry, prompting the rapid development of solutions designed to circumvent these bottlenecks. Notably, several commercial systems now boast the capability to complete a full PCR run in a mere minute or so, albeit often on a limited number of samples. This unprecedented speed is perfectly suited for point-of-care (POC) applications, bringing diagnostic capabilities closer to patients and enabling quicker clinical decisions. Yet, a crucial challenge persists: most of these rapid PCR systems primarily operate on the principle of end-point PCR, which necessitates an additional, often time-consuming, post-amplification analysis step. Traditional methods for analyzing PCR products, such as gel electrophoresis, while robust, are fundamentally incompatible with the stringent time and resource constraints inherent to a POC setting. Consequently, there is a burgeoning and critical need for fast, user-friendly, and accessible methods for directly analyzing PCR products outside of a centralized laboratory.

The pandemic also highlighted the unparalleled relevance of lateral flow assay (LFA) technology, showcasing its speed, simplicity, and ease of use through the widespread adoption of rapid antigen tests. While many popular LFA systems are specialized commercial products, such as lateral flow immunoassays for human chorionic gonadotropin in pregnancy tests or for the SARS-CoV-2 nucleocapsid N protein in COVID-19 diagnostics, these typically involve custom-designed chromatographic labels and test strips specific to a single target. However, this approach represents an exception rather than the norm in the broader biosensing landscape. For the sake of sustainability and broad applicability, most established biosensing technologies, such as immunostaining or Enzyme-Linked Immunosorbent Assay (ELISA), rely on universal labeling units, often based on a universal secondary antibody. In the realm of amplicon detection, nucleic acid-based lateral flow assays (NALFAs) have emerged as a promising avenue for rapid and visual detection of amplicons, offering a compelling alternative to traditional post-amplification analysis methods [1]. These assays already commonly leverage a universal detection scheme where one PCR primer is modified with biotin and the other with a distinct antigen, such as digoxigenin or fluorescein, facilitating capture or detection via corresponding antibodies [2]. While this antibody-mediated approach provides a degree of universality, recent advancements have also explored antibody-free NALFA formats to overcome the complexities and potential limitations associated with immunoassays in this context [3], thereby simplifying the assay design and potentially reducing manufacturing costs.

Furthermore, the field of genetic material detection has seen the innovative application of intrinsically multiplexable anisotropic particles, such as gold nanorods, which offer unique optical properties for signal generation and readout [4]. Many modern genosensing protocols, particularly in areas like gene expression profiling or identifying panels of pathogens, require the simultaneous detection of multiple genes. To enable robust multiplexing within an LFA format, possible strategies include either spatial segregation of distinct test lines or the development of orthogonal dimensions, such as color. The latter approach necessitates different detection units alongside plasmonic labels of distinct colors, thereby

requiring a solution to overcome the usual reliance on single-color (typically pink) gold nanospheres. In this context, gold nanorods represent an outstanding solution in terms of sustainability and versatility due to their tunable surface plasmon resonance, allowing for the generation of various colors depending on their aspect ratio.

Our current work directly addresses the emerging need for rapid PCR product analysis by aiming to develop a novel technology for the readout of PCR amplicons based on the lateral flow format. Beyond mere speed and ease of use, our vision extends to preserving key features generally indispensable in genosensing applications, specifically focusing on universality, multiplexing, and quantitative readout capabilities. Our approach leverages the inherent customizability of PCR primers to create an antibody-free NALFA system. We implement our previously conceived idea by modifying the forward primer with a universal, multiplexable, genetic barcode, which is also immobilized on the control line of the LFA strip. Concurrently, the reverse primer is modified with biotin. We then functionalize our plasmonic labels, made of inherently multiplexable gold nanorods, with the anti-barcode sequence and immobilize streptavidin on the test line of the LFA strip. This unique design allows plasmonic staining of the test line only when forward and reverse primers are bound together, signaling successful, specific amplification into amplicons. Crucially, all ingredients present on the LFA strip remain universal and multiplexable, allowing for broad applicability across different target genes without the need for redesigning the entire assay.

We will demonstrate the initial feasibility of our integrated system through the detection of a model gene, *rolC*, an oncogene of significant botanical interest. The *rolC* gene, originating from *Agrobacterium rhizogenes*, is known to drastically alter plant growth and development by encoding a cytokinin-β-glucosidase. This enzyme releases active cytokinins from their glucoside conjugates, thereby disrupting plant hormone balance and inducing specific phenotypic changes, often associated with tumor formation or altered secondary metabolite production in transgenic plants. This makes *rolC* an ideal and well-characterized target for validating our genosensing platform. Furthermore, we aim to showcase the potential of our system for quantitative analysis by integrating it with a common smartphone video camera and a basic machine learning pipeline for immediate signal interpretation. This approach promises to provide a portable, cost-effective, and rapid solution for PCR amplicon detection and quantification, particularly valuable for POC diagnostics and field-based applications.

Materials and Methods

1. Materials

All chemicals for the synthesis of gold nanorods, including cetyltrimethylammonium bromide (CTAB), tri-sodium citrate dihydrate (Na3-citrate), Tween 20, tris(2-carboxyethyl)phosphine hydrochloride (TCEP), sodium chloride (NaCl), low EEO agarose, tris–borate EDTA (TBE) buffer, DirectLoad™ 50 bp DNA step ladder, 6 × DNA loading buffer, GelGreen® Nucleic Acid Stain, sodium dodecyl sulfate (SDS), phosphate-buffered saline (PBS), and all reagents needed for PCR amplification were purchased from Merck (Merck KGaA, Germany). Unmodified, A18-barcoded and biotin-labelled PCR primers were obtained from Eurofins Genomics (Eurofins Scientific, Germany) and the thiolated T18 tag sequence from metabion (metabion international AG, Germany). Materials for the assembly of the lateral flow assay included a sample pad, a conjugate pad, a nitrocellulose membrane for the test and control lines, and an absorbent pad.

2. Synthesis and Bio-conjugation of Gold Nanorods

Cetrimonium-coated gold nanorods were prepared following the protocols described by Ye et al.. The cetrimonium was then gradually replaced with citrate according to the procedure reported in our recent work [DOI: 10.1007/s11051-024-06211-z]. Citrate-coated gold nanorods were bio-conjugated with a synthetic T18 oligonucleotide modified with a thiol group at its 3′-end, after treatment with 10 mM TCEP for 1 h at room temperature. The particles (0.8 mM Au) were incubated with the poly-T filament (approximately 4 μM) at 4 °C in 0.5 mM Na3-citrate and 0.005% Tween 20. NaCl was slowly added over 2 days until a final concentration of 1 M was reached. The suspensions were then washed four times to remove any unbound oligonucleotide and reconstituted in a ready-to-use hybridization buffer (DIG Easy Hyb™, Roche Diagnostics, Germany).

3. Preparation, Amplification, and Characterization of DNA Targets

The cloning vector used as a template for PCR amplification of the rolC gene was pUC19 (2686 bp, New England BioLabs®, USA). A 1860-bp *Agrobacterium rhizogenes* (strain 1855) HindIII-EcoRI restriction fragment, encompassing both the promoter and the coding region of the rolC gene (ORF12, 308 bp), was cloned into the pUC19 polylinker restriction sites and ligated with T4 DNA ligase (New England BioLabs®, USA). The recombinant vector was then transformed into *E. coli* One Shot Mach 1™-T1 (Thermo Fisher Scientific, USA) highly competent cells. Plasmids were extracted from the recombinant clones, verified by digestion with HindIII-EcoRI restriction enzymes, and subsequently used as templates in PCR reactions.

Specifically, templates (approximately 1 ng) were amplified by end-point PCR (T100™ Thermal Cycler, Bio-Rad Laboratories, USA) with specific unmodified, A18-barcoded, and biotin-tagged primers (200 nM) at an annealing temperature of 55 °C. The reactions were carried out in the presence of 0.8 mM dNTPs and 0.05 U/μl JumpStart™ Taq DNA Polymerase (Sigma-Aldrich®, Merck KGaA, Germany), for 45 cycles in several replicates. Purification of the PCR products was performed using MicroSpin columns (illustra™ GFX PCR DNA and gel band purification kit, GE Healthcare, UK), by eluting the samples with 10 mM Tris–HCl buffer (pH 8.0). Their concentration was quantified using a Qubit fluorometer (Invitrogen, Thermo Fisher Scientific, USA).

To verify the effective modification of the amplicons with poly-A and biotin tails at the end of one or both strands, each sample was subjected to agarose gel electrophoresis (1.6% in 0.5 × TBE buffer) at 100 V for 90 min. The various DNA bands were detected with GelGreen® nucleic acid dye under a blue LED light transilluminator (MaestroGen UltraSlim LED Transilluminator, MaestroGen Inc., Taiwan), and their molecular weights were compared against a 50 bp DNA marker (DirectLoad™ 50 bp DNA step ladder, Sigma-Aldrich®, Merck KGaA, Germany).

4. Lateral Flow Assay Strip Preparation and Recording

The lateral flow assay strip was prepared according to a typical scheme. T18-modified gold nanorods were dispensed onto the conjugate pad. The test pad was immobilized with a single spot of streptavidin at the test line. The control spot on the test pad contained a single spot of streptavidin combined with biotinylated A18. The strip was then assembled into a home-made cassette constructed from PMMA, encompassing a hole for sample application onto the sample pad and an inspection window over the test pad. The assembled cassette was placed onto a lightboard from a typical producer. A volume of 80 μL of amplicons, at concentrations ranging from 75 ppb to 10 ppm and a zero concentration control, was applied onto the sample pad. The system's progression was recorded as a movie using the posterior 50MP camera of a realme GT 2 smartphone device, mounted onto a simple easel.

5. Quantitative Data Analysis

To assess the feasibility of analyzing the acquired movies within the framework of a supervised machine-learning problem, we evaluated the sensitivity of a pipeline designed to receive a time-lapse movie of the assay as input and provide a quantitative prediction of the amplicon concentration as output. Due to the extreme limitation of the available dataset (n = 36 instances at 18 different amplicon concentrations), a strong reduction of its dimensionality, a preference for the simplest possible model, and a workflow circumventing the need for splitting into training and testing sets were necessary. Our primary objective was to understand the relevance of machine learning in our system, rather than to deploy an operational predictor.

For dimensionality reduction, image segmentation, and feature selection, movies were first resized to grayscale, 1 frame per second, and 145 x 260 pixels. They were then preprocessed using a tool that extracts the relative image contrast over a region of interest encompassing the location immediately upstream and downstream of the forming test spot. Relative contrast-over-time plots were constructed and fitted to a two-segment piecewise linear function to reduce noise and retain the nonlinear content of the original data. From these fitting curves, a set of data was extracted every 50 frames from the onset of wicking in the region of interest, which was identified as a sharp peak of relative contrast. These data were used as input to feed the machine learning algorithm with a vector of length m = 6 dimensions per instance.

For the supervised machine learning analysis, we used Scikit-learn as a high-level environment comprising tools for performance assessment. Specifically, we tested the simplest model of a linear regressor and calculated its performance metrics using a cross-validation analysis implemented with a leave-one-out strategy (an extreme case of K-fold cross-validation with K = n). For each K-fold iteration, Scikit-learn provides both a test and a training error, which we compared for an overall assessment of its generalization error. We also used the cross-validation tool to generate so-called clean predictions, where the concentration of each instance was inferred from a sub-model trained with all other 35 cases. These predictions were examined to identify relevant trends versus true concentration and to gain an indicative estimate of the sensitivity of our simple predictor. However, we declined to deploy and fully test a complete regressor due to the small size of the available dataset.

Results and discussion

Citrate-stabilized gold nanorods were successfully functionalized with thiolated oligonucleotides via a salt aging protocol, a method commonly employed for nanospheres. This technique, involving a gradual increase in ionic strength, proved instrumental in promoting robust colloidal stability and achieving efficient oligonucleotide loading onto the nanoparticles. Specifically, modification with an 18-mer polythymine (T18) oligonucleotide provided excellent colloidal stability in saline buffers, consistent with our previous work (doi: 10.1038/s41598-022-10227-7).

A lateral flow genoassay was subsequently developed for the detection of *rolC* amplicons. These amplicons were generated using a commercial end-point thermocycler with a plasmidic template, employing a forward primer functionalized with an 18-mer polyadenine (A18) barcode and a biotinylated reverse primer, under otherwise standard conditions. Post-amplification, the amplicons were analyzed by gel electrophoresis, then purified and quantified by spectrophotometry.

[Figure on particles and amplicons]

With these amplicons, the universal detection strategy relied on colloidal gold nanorods functionalized with the complementary T18 sequence, deposited onto the conjugate pad. The detection pad featured streptavidin immobilized at the test (T) location and a streptavidin-conjugated biotinylated A18 barcode at the control (C) location. A key advantage of this design is the universality of the entire device, allowing for adaptation to various genetic targets. The assay's mechanism involves the binding of target amplicons to the modified nanoparticles via A18-T18 hybridization, leading to their capture at the test line via biotin-streptavidin coupling. Unbound nanoparticles, in turn, hybridize with the A18 barcode at the control line.

Figure X illustrates the specificity analysis of the developed lateral flow amplicon assay for *rolC*. Gold nanorods conjugated to polythymine were used on the conjugate pad, with streptavidin at the test (T) spot and a polyadenine-biotin-streptavidin hybrid at the control (C) spot. A volume of 80 µL of approximately 2 ppm amplicon was applied for each test. The results were as follows: (1) The negative control, containing no amplicon, yielded no staining at the test line. (2) Unmodified *rolC* amplicon similarly produced no staining at the test line, confirming the requirement for specific primer modifications. (3) The positive control, A18-*rolC*-biotin amplicon, exhibited clear staining at the test line, validating the detection mechanism. (4) Application of A18-*rolC* amplicon (lacking the capture probe ligand, biotin) resulted in no test line staining. (5) Similarly, *rolC*-biotin amplicon (lacking the detection probe ligand, A18 barcode) also showed no test line staining. Crucially, consistent staining was observed at the control line in all tested cases, confirming proper fluidic flow and reagent functionality.

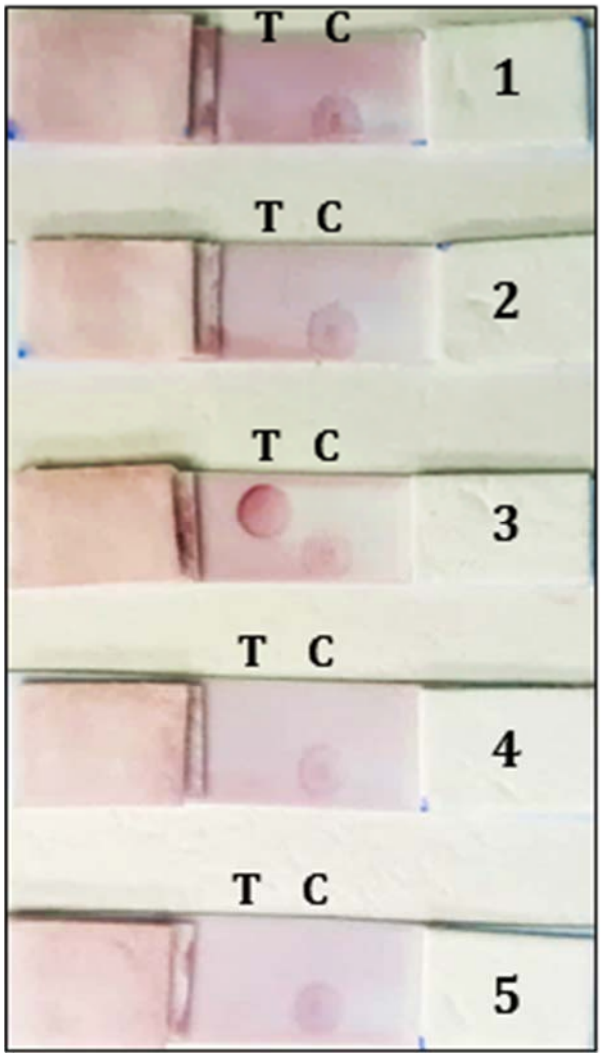

Figure X...

We further explored the potential for quantitative analysis using a smartphone camera. Videos of lateral flow assays performed in standardized cassettes were captured. Our hypothesis was that analyzing the colorimetric development kinetics could extend the dynamic range of the assay beyond simple endpoint visual assessment. A dataset comprising 36 videos, spanning various target amplicon concentrations, was acquired. To reduce data dimensionality, we tracked the image contrast over the test area, specifically evaluating regions upstream and downstream of the developing test spot. Plots of contrast-over-time typically revealed a sharp peak at the initiation of wicking, which served as a robust temporal marker. This initial peak was consistently followed by a growth phase, although its sub- or superlinear nature could not be definitively correlated with any specific experimental parameter within this dataset.

To further minimize dimensionality and mitigate noise, the kinetic data were fitted to a two-segment piecewise linear function. Image contrast values at predefined time points subsequent to the wicking marker were then extracted for analysis.

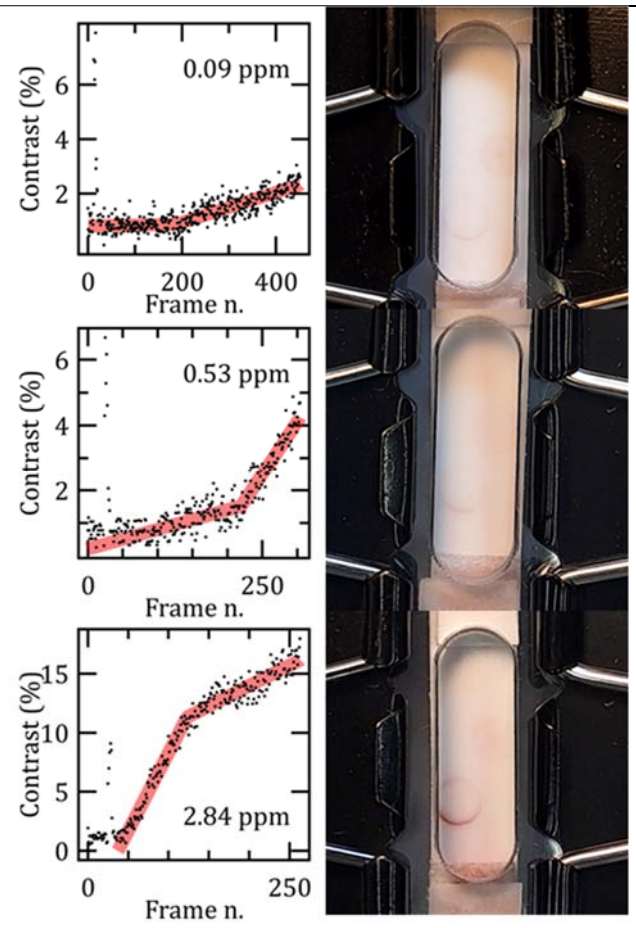

Figure Y...

Given the limited size of the dataset, a hyperparameter-free linear model was selected and trained using these extracted contrast values via SciKit-learn. A leave-one-out cross-validation strategy was implemented, involving 36 individual regressors, each trained on 35 instances and used to generate "clean" predictions for the excluded instance. The correlation between these predictions and the actual quantitative labels is graphically presented in Figure Y. This comprehensive validation allowed for a thorough analysis of the validation error and the estimation of the system's sensitivity, which was determined to be approximately 300 ppb. This sensitivity is comparable to that achievable through visual assessment. However, the observation of a 30% increase in validation error relative to the training error suggests potential overfitting, despite the inherent simplicity of the chosen linear model. Therefore, future work will focus on acquiring a significantly larger dataset to further improve model performance and robustness.

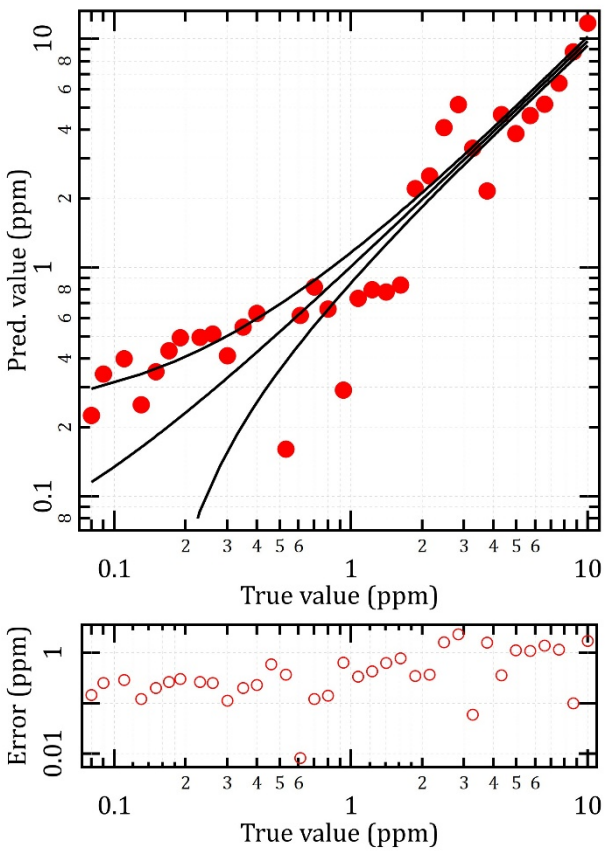

Figure Z...

Our developed universal lateral flow system for amplicon detection demonstrates overall robust functionality and performs as anticipated. A particularly noteworthy and non-trivial aspect was the inherent compatibility of the kinetics driven by capillary action with those governing oligonucleotide hybridization and biotin-streptavidin coupling. This is significant because, in our previous work, we observed that similar molecular recognition systems typically required tens of minutes to react when performed in solution or in a static dot-blot format. The accelerated flow through the porous lateral flow membrane appears to be a key factor in enhancing the kinetics of molecular recognition by mitigating the limitations imposed by molecular diffusion. Nevertheless, it remains imperative to highlight several aspects that warrant further development or raise points for consideration for future optimization.

Foremost, to achieve optimal system performance, we found it necessary to purify the amplicons and transfer them into a dedicated buffer. This critical step served a dual purpose: to effectively remove unreacted excess primers and to mitigate the incompatibility observed between the standard end-point PCR buffers and our lateral flow platform. Although this purification step does not represent an insurmountable technical barrier, it unequivocally constitutes a limitation for real-world point-of-care (POC) applications. For a truly integrated and user-friendly POC diagnostic, seamlessly incorporating the functions of purification and buffer exchange directly into the paper-based microfluidic platform is essential. While the scientific literature abounds with excellent examples of paper-based microfluidic systems specifically designed for on-chip sample purification and buffer exchange (e.g., [Reference 1: e.g., Zhang, T., et al. "Paper-based microfluidic devices for biological sample preparation." *Lab on a Chip* 13.21 (2013): 4016-4024.] or [Reference 2: e.g., Martinez, A.W., et al. "Diagnostics for the developing

world: microfluidic paper-based analytical devices." *Analytical Chemistry* [1] 82.1 (2010): 3-10.]), this integration remains a pivotal area for future implementation in our ongoing work.

Another aspect that currently eludes a complete explanation is the observed kinetic behavior of color development at the test line, which exhibits both sublinear and superlinear profiles across different assays. This variability suggests underlying mechanisms or influencing factors that are not yet fully understood and warrant deeper investigation into the binding dynamics and optical readout processes.

Furthermore, our current approach to test strip production heavily relies on manual fabrication. We hypothesize that a greater level of automation in material manufacturing, particularly through the use of dedicated spotters for the precise deposition of reagents at the test and control lines, would significantly enhance the reproducibility of the system. Improved manufacturing consistency is expected to directly translate into superior performance for quantitative analysis, a critical feature for diagnostic applications. This move towards automation would standardize reagent distribution and potentially minimize the observed kinetic variations, leading to more consistent and reliable quantitative readouts.